Ch 14
Emulsions

Emulsions

Dispersion of one fluid in another

-> a liquid foam, which is typically a dispersion of 95% air in liquid, acts as an elastic solid, with a yield stress and a finite zero-frequency modulus

-> stability of the dispersed phase against coagulation or clumping is a major concern

Emulsion preparation

1. Mechanical mixing
2. Phase separation; by a thermal quench or by a chemical reaction

-> control of the emulsion morphology is a delicate business because the emulsified state is at best only kinetically, and not thermodynamically stable

Phase separation

UCST; upper critical solution temperature

the critical temperature above which the two components are miscible, and below which there is a coexistence region of two-phase equilibrium

LCST; lower critical solution temperature

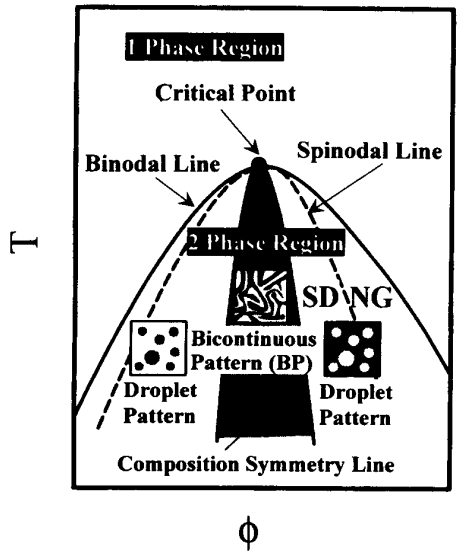

Figure 9-1 Schematic phase diagram of a binary fluid mixture of small molecules. The two-phase region lies under the binodal line, the apex of which defines the critical temperature T_c and critical composition ϕ_c. Between the binodal and the spinodal lines, phase separation is by nucleation and growth (NG), while under the spinodal line it is by spinodal decomposition (SD). Within the region of spinodal decomposition, near the compositional symmetry line, there is a region where the morphology is initially bicontinuous. Outside of this region, one of the phases is a discontinuous droplet phase. Eventually, because of asymmetries, initially bicontinuous structures break apart into a droplet morphologies. (From Tanaka 1995, reprinted with permission from the American Physical Society.)

Asymmetric phase diagram

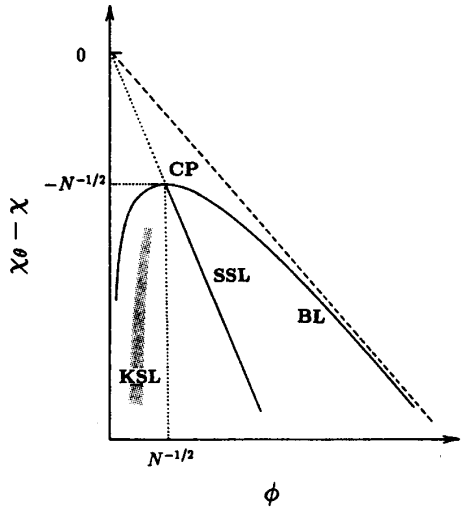

Figure 9.2 Schematic phase diagram of a polymer/solvent mixture, where χ is the Flory "chi" parameter, and $\chi_\theta = 1/2$ is χ at the theta temperature. The quantity $\chi_\theta - \chi$ along the ordinate is a reduced temperature, and ϕ is the polymer volume fraction. CP is the critical point, and BL is the binodal line. SSL and KSL are the static symmetry line and the kinetic symmetry line, respectively. These lines define the phase-inversion boundaries during quenches. In quenches that end at the right of such a line, the polymer-rich phase is the continuous phase, while to the left of the line the solvent-rich phase is the continuous one. SSL applies at long times, after viscoelastic stresses have relaxed, while KSL applies at shorter times before relaxation of viscoelastic stresses. (From Tanaka 1993, reprinted with permission from the American Physical Society.)

Phase separation

The dynamics of the separation process depends on
- final temperature T_f
- composition
- the rate of quench dT/dt
- viscoelastic properties of the phases formed
- interfacial tension

Two generic types of phase separation

1. Spinodal decomposition (SD);
   when the mixture is quenched into a part of the phase diagram where the mixture is unstable to small variations in composition, leading to immediate growth of phase-separated domains
2. Nucleation and growth (NG);
   when the mixture is stable to small compositional variations, but not to large ones, then phase separation is suppressed until a nucleus of one phase forms that is large enough to be unstable to further growth

Free engergy composition diagram

If $T<T_c$ and the composition lies between the two minima ϕ_1, ϕ_2 the mixture can lower its free engergy by phase separating into two phases whose compositions are ϕ_1, ϕ_2

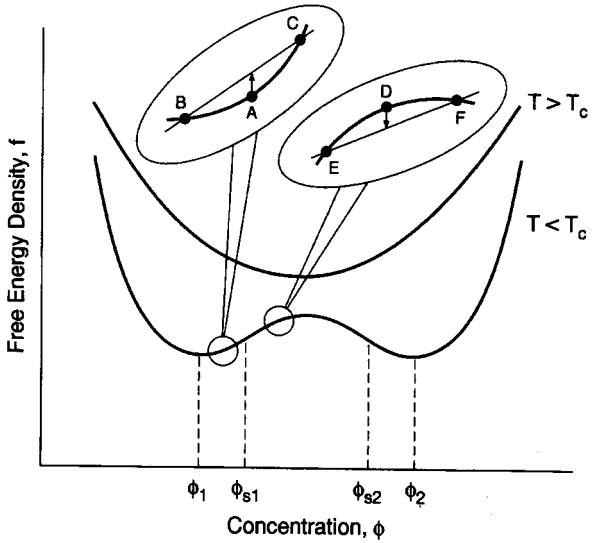

Figure 9.3 Schematic drawing of free energy versus concentration for a binary mixture at temperatures above and below the critical value T_c. The concentrations ϕ_1 and ϕ_2 are the equilibrium binodal concentrations, while ϕ_{s1} and ϕ_{s2} are the spinodal concentrations. As illustrated in the insets, at a homogeneous concentration between ϕ_1 and ϕ_{s1}, a concentration fluctuation leads to an *increase* in free energy, while at a concentration between ϕ_{s1} and ϕ_{s2}, a fluctuation leads to a *decrease* in free energy.

When the curvature *f"*>*0*, a weak compositional fluctuation increases average free energy -> the fluctuation is unfavorable -> homogenous composition is restored (NG) -> nucleus in the delayed period is metastable

When the curvature *f"*<*0*, decrease of free engergy -> weak fluctuation grows spontaneously until two distinct phases appear (SD)

Spinodal decomposition

The stages of SD following a sudden drop in temperature

1. Early stage;
   a small amplitude sinusoidal composition wave develops, and the amplitude of this wave grows exponentially in time, while the wavelength stays almost constant

2. Intermediate stage;
   the amplitude of the wave continues to grow, but at a less-than-exponential rate, and the wavelength of the pattern begins to increase

3. Transition stage;
   the wave becomes highly nonsinusoidal; the maximum and minimum concentrations reach equilibrium values, but the interfaces have not yet thinned to their final widths

4. Late stage;
   there are well-defined domains; neither the interfacial width nor the composition change much with time, but the domain sizes keep increasing as the pattern coarsens

Spinodal decomposition

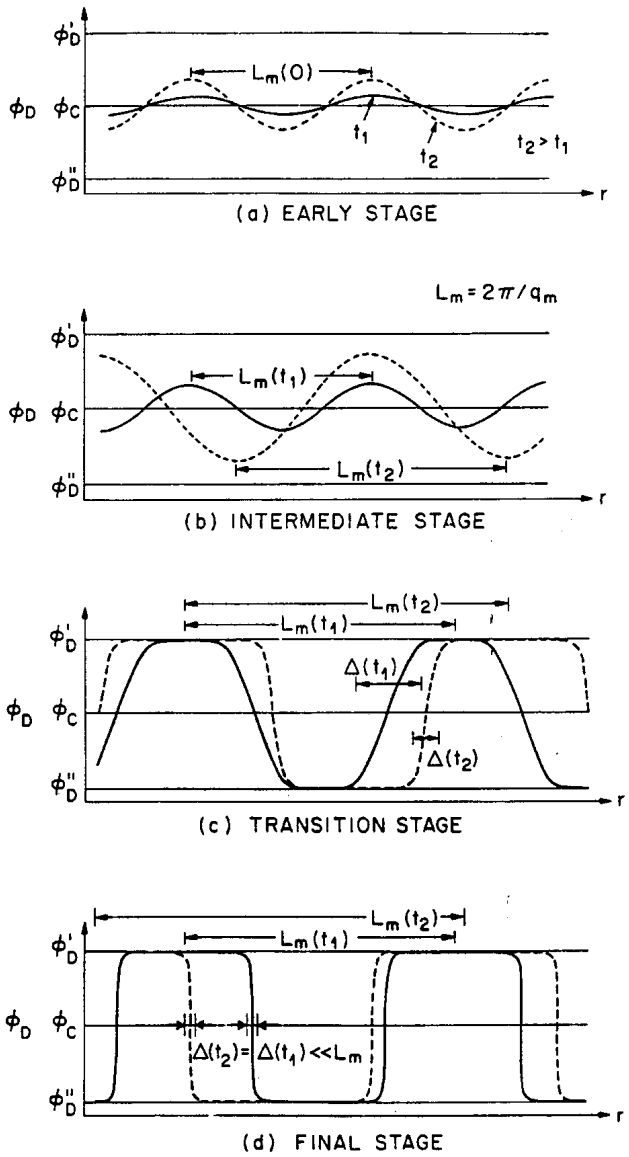

Figure 9.4 Four stages of spinodal decomposition, according to Bates and Wiltzius (1989). In each diagram, the dashed line represents the composition profile at a later time, t_2, than that for the solid line, t_1. The compositions ϕ'_D and ϕ''_D are the equilibrium compositions in the two phases. In the early stage **(a)**, the wavelength L_m of the sinusoidal pattern remains constant, while the amplitude increases. In the intermediate stage **(b)**, both the amplitude and the wavelength increase with time. In the transitional stage **(c)**, the amplitude is saturated and no longer changes with time, but the wavelength increases, and the width Δ of the interfacial zone decreases, with time. In the final or "late" stage **(d)**, the amplitude is constant and so is the interfacial width Δ, and only the wavelength of the pattern increases with time. (From Bates and Wiltzius, reprinted with permission from J. Chem. Phys. 91:3258, Copyright © 1989, American Institute of Physics.)

Mechanical mixing

When agitation ceases, unless surfactants are present, interfacial tension drives the two phases back toward separation; by droplet-droplet collision and fusion, by sedimentation or creaming; by Ostwald ripening (coarsening to reduce the interfacial area and the total free engergy)

Size distribution of the droplets should be controlled; it is affected by;
shear rate, flow type, surface tension, flow history, viscosity ratio, driplet inertia, fluid composition, non-Newtonian effect, and so on

Droplet breakup in emulsions

$$\mathrm{Re} = \rho_d \dot{\gamma} a^2 / \eta_s$$

If gravitational settling can be neglected, and if the droplet Reynolds number is small, then the droplet deformation and possible breakup are controlled by two dimensionless groups; Capillary number *Ca* and viscosity ratio *M*

$$Ca \equiv \frac{\dot{\gamma}\eta_s a}{\Gamma} \qquad M \equiv \frac{\eta_d}{\eta_s}$$

For small deformation, the droplet deformation *D* is predicted (by Taylor)

$$D = Ca \cdot f(M) \qquad f(M) \equiv \frac{19M + 16}{16(M + 1)} \qquad D \equiv \frac{L - B}{L + B}$$

Droplet breakup occurs when the viscous stresses that deform the droplet overwhelms the surface tension forces that resist deformation

$$D_b \approx f(M) \cdot Ca \approx 0.5$$

Refinements to Taylor theory

When the viscosity ratio is low, $M<0.05$, the droplets deform greatly before they break

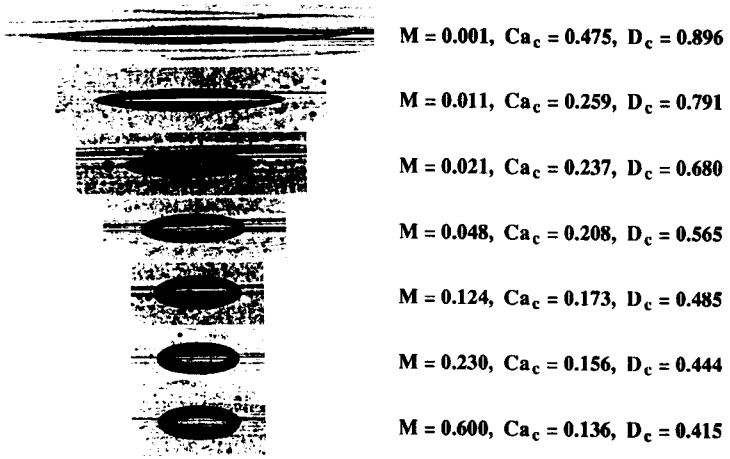

Figure 9.7 Photographs of droplet shapes in planar extensional flow for various viscosity ratios M of the dispersed to the continuous phase. The droplets are viewed in the plane normal to the velocity gradient direction. The critical capillary numbers Ca_c and droplet deformation parameters D_c at breakup are also given. The droplet fluids are silicon oils with viscosities ranging from 5 to 60,000 centistokes, while the continuous fluids are oxidized castor oils; both phases are Newtonian. (From Bentley and Leal 1986, with permission from Cambridge University Press.)

Refinements to Taylor theory

At low M, highly elongated droplets have pointed ends from which tiny 'satellite' droplets are in some cases ejected

At high M, droplet deformation remains modest and no breakup is observed even at high capillary number

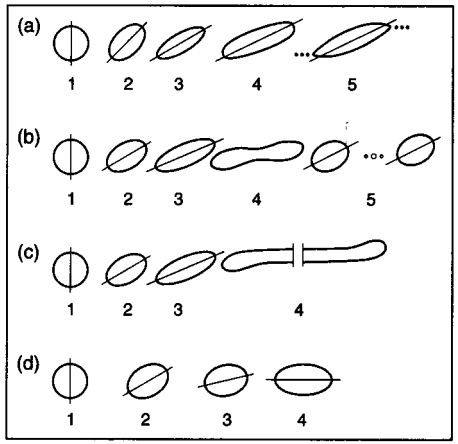

Figure 9.8 Tracings of droplet shapes in shearing flows showing changes of shapes and orientations of droplets as the shear rate increases from left to right. Here the droplets are visualized in the plane containing the velocity and the velocity-gradient directions. **(a)** $M = 2 \times 10^{-4}$: a droplet of water in 52.6 P silicone oil; **(b)** $M = 1$: a droplet of oxidized castor oil in 52.6 P silicone oil; **(c)** $M = 0.7$: a droplet of oxidized castor oil in corn syrup; and **(d)** $M = 6$: a droplet of viscous silicon oil in oxidized castor oil. In **(a)**, picture 5, tiny satellite droplets are spit from the droplet tips. In **(b)**, picture 4, a neck forms which breaks as shown in picture 5, leaving two droplets plus three satellite droplets. In **(c)**, picture 4, the droplet is stretched into a long filament (possibly because of interfacially active ingredients in the corn syrup). In **(d)**, no droplet bursting is seen. (From Rumscheidt and Mason 1961, reprinted with permission from Academic Press.)

Critical conditions for droplet breakup

$$Ca \equiv \frac{G\eta_s a}{\Gamma}$$

over a wide range of capillary number, viscosity ratio, and flow types

$$\nabla \mathbf{v} = \frac{1}{2} G \begin{pmatrix} 1+\alpha & 1-\alpha \\ -(1-\alpha) & -(1+\alpha) \end{pmatrix}$$

G; shear rate for shear flow(α=0), extension rate for planar extensional flow(α=1)

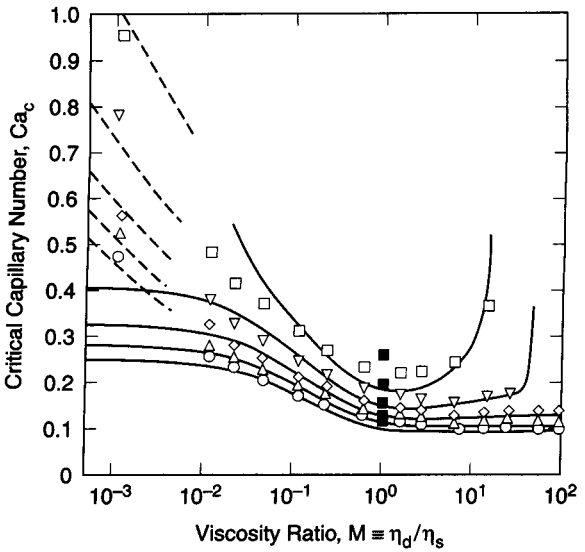

Figure 9.9 Dimensionless critical droplet size for breakup (capillary number $Ca_c \equiv G\eta_s a/\Gamma$) as a function of viscosity ratio M of the dispersed to the continuous phase for two-dimensional flows in the four-roll mill. The data sets correspond from bottom to top to $\alpha = 1.0$ (◯), 0.8 (△), 0.6 (◇), 0.4 (▽), and 0.2 (□), with α defined in Eq. (9-17). The fluids are those described in Fig. 9-7. The solid lines are the predictions of a small-deformation theory, while the dashed lines are for a large-deformation theory. The closed squares are from Rallison's (1981) numerical solutions (see also Rallison and Acrivos 1978). (From Bentley and Leal 1986, with permission from Cambridge University Press.)

Droplet coalescence in emulsions

The coalescence and breakup occur simultaneously, produce different steady-state droplet sizes

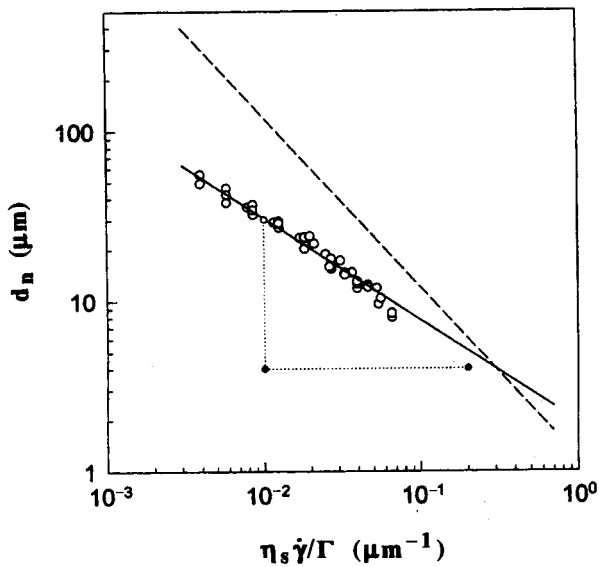

Figure 9.10 Number-average drop diameter as a function of $\eta_s\dot{\gamma}/\Gamma$ for blends of 10% polyisobutylene in polydimethylsiloxane with $M = 0.47$. The solid line is the prediction of the Janssen theory, and the dashed line is for the Taylor theory with $Ca_c = 0.6$. The dotted line connecting two solid symbols shows a "trajectory" when the shear rate is suddenly reduced. (From Grizzuti and Bifulco 1997, reprinted with permission from Steinkopff Publishers.)

Critical average droplet diameter above which both breakup and coalescence occur

$$d_c = \frac{8}{\sqrt{3}} Ca_c^{-3/2} M^{-5/3} h_c$$

Coalescence is more important for immiscible polymer blends than for low-viscosity liquids under shear

Droplet dynamics in immiscible polymer blends

It is important to understand and control the size and shape of the particles of dispersed pahse, because the properties depend on them

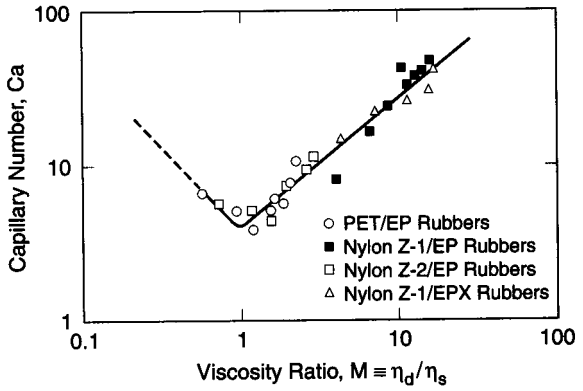

Figure 9.11 Dimensionless droplet size (capillary number) as a function of viscosity ratio M for various blends of 15 wt% ethylene–propylene rubbers in nylon or polyester produced by extrusion at an "effective shear rate" of around 100 sec^{-1}. The components are shear thinning, and the viscosity ratio M is evaluated at the "effective shear rate." (From Wu 1987, reprinted with permission from the Society of Plastics Engineers.)

$$a = \frac{2\Gamma M^{\pm 0.84}}{\dot{\gamma}\eta_s}$$

+ sign in the exponent applies when $M>1$, and – when $M<1$

This empirical expression was obtained using blends for which the dispersed phase concentration was 15% by weight and the effective shear rate was 100 sec^{-1}

As the viscosity is shear rate dependent, the viscosities are taken to be those of the melts at a nominal shear rate in the mixer

Droplet dynamics in immiscible polymer blends

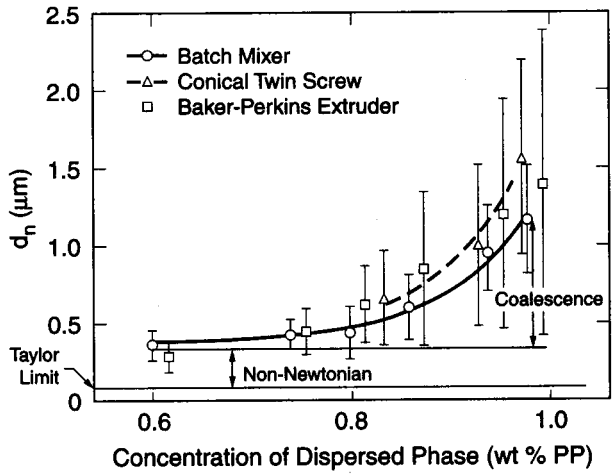

Figure 9.13 Number averaged diameter of droplets d_n of polypropylene ($M_n = 60{,}000$) in polystyrene ($M_w = 200{,}000$) as a function of wt% polypropylene mixed in three different mixers at a nominal shear rate of around 65 sec^{-1} and $T = 200°C$. The viscosities of the the PP and PS under these conditions are 840 and 950 Pa·s, respectively. The interfacial tension Γ is 5.0 dyn/cm. The "error bars" represent the distribution of droplet sizes, and they encompass one standard deviation in each direction from the mean. The deviation from the Taylor limit at low concentrations is attributed to non-Newtonian effects, while the increase in droplet size at higher concentrations is attributed to droplet coalescence. Note that similar droplet sizes are obtained in all three different mixers. (Reprinted with permission from Sundararaj and Macosko, Macromolecules 28:2647. Copyright © 1995, American Chemical Society.)

Elasticity suppresses droplet breakup like interfacial tension;

The droplet radius at break up becomes $a_c = \dfrac{\Gamma \cdot Ca_c}{\eta_s \dot{\gamma} - N_1(\dot{\gamma})}$